# The general promoting effect of polydopamine on supported noble metal catalysts

*Mingwei Zhang, Guozhu Li*, Xiaoqing Sun, Yujiao Jiang, Xiangwen Zhang*

Key Laboratory of Green Chemical Technology of Ministry of Education, Collaborative Innovation Center of Chemical Science and Engineering (Tianjin), School of Chemical Engineering and Technology, Tianjin University, Tianjin 300072, PR China.

* Corresponding author.

Tel.: +86 22 27892340

E-mail: gzli@tju.edu.cn

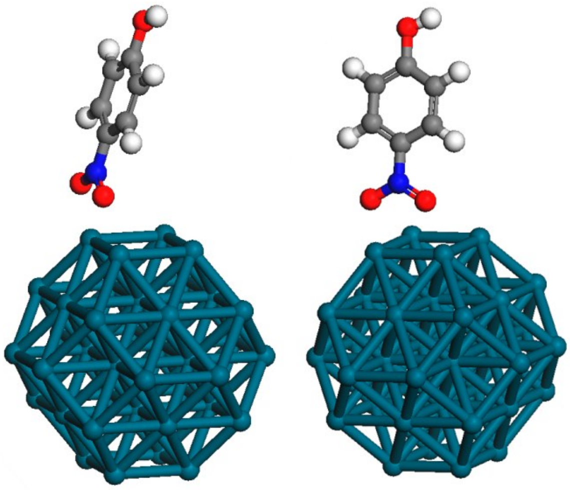

**Figure S1.** Chosen binding geometry for 4-NP chemisorption on a 38-atom Pd nanoparticle (left: side view, right: front view).

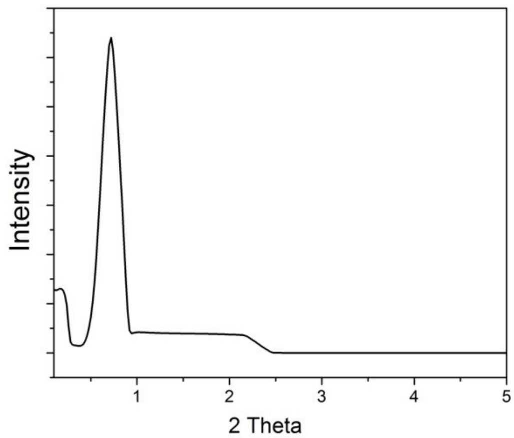


**Figure S2**. Small angle XRD pattern of SBA-15.

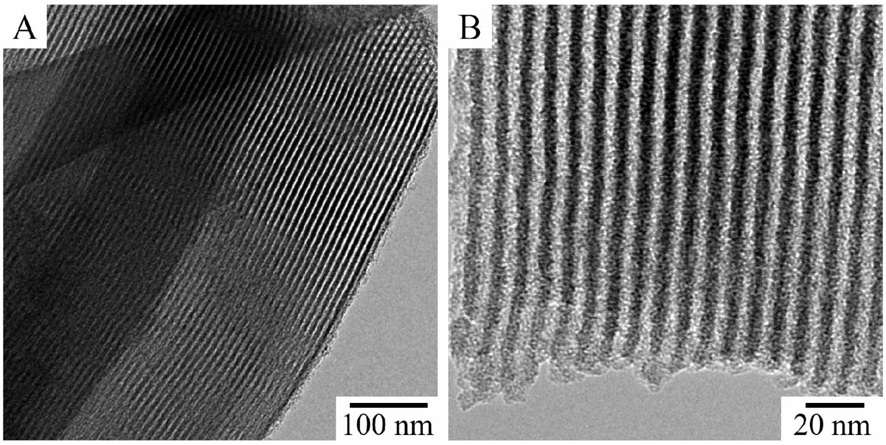


**Figure S3**. TEM images of SBA-15.

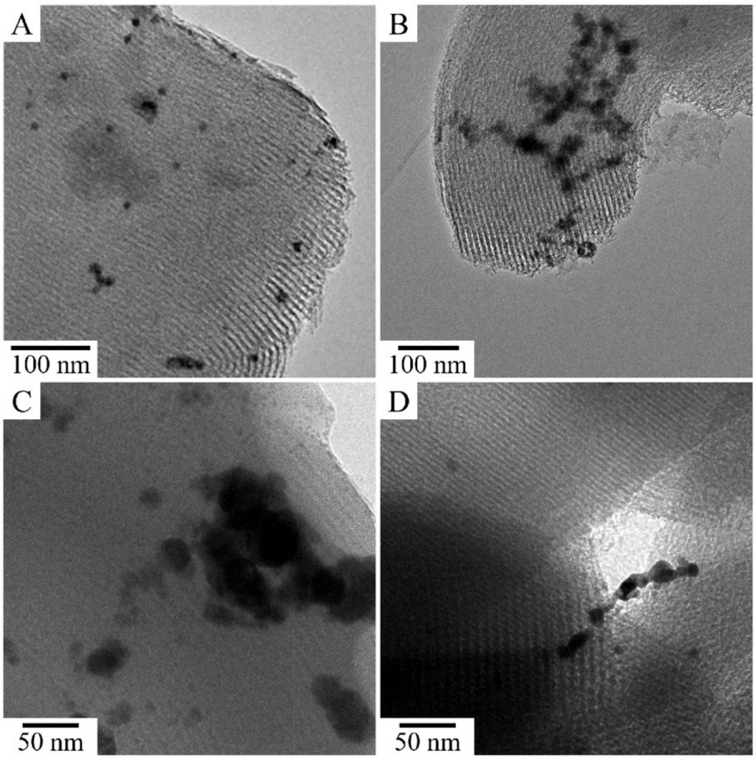


**Figure S4**. TEM images of the as-synthesized Pt/SBA-15 (A), Pd/SBA-15 (B) Ag/SBA-15 (C) and Au/SBA-15 (D) by traditional method. Scale bar is 100 nm for (A) and (B), and 50 nm for (C) and (D).

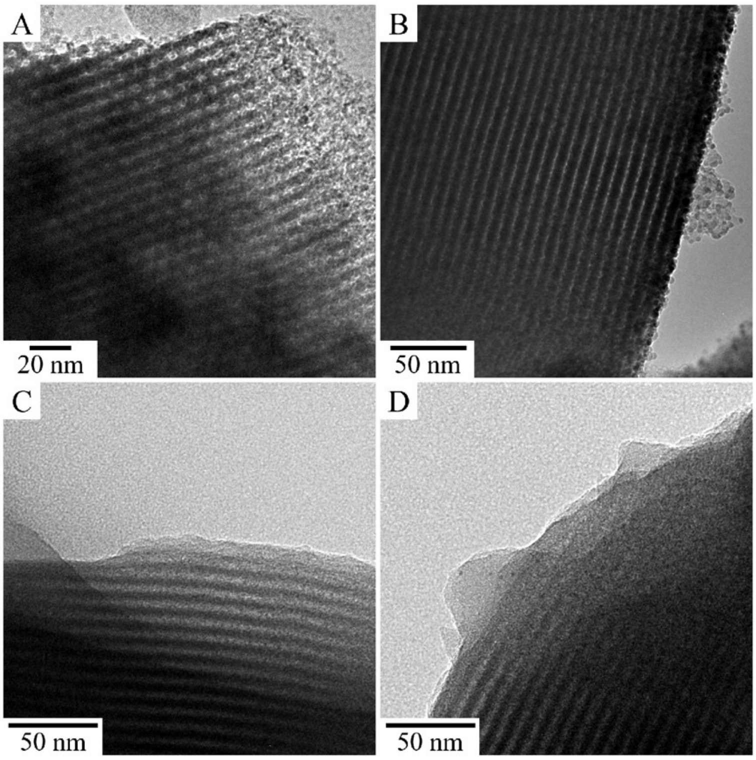


**Figure S5**. TEM images of the as-synthesized Pt/DA-SBA-15 (A), Pd/DA-SBA-15 (B), Ag/DA-SBA-15 (C) and Au/DA-SBA-15 (D). Scale bar is 20 nm for (A) and 50 nm for (B), (C) and (D).

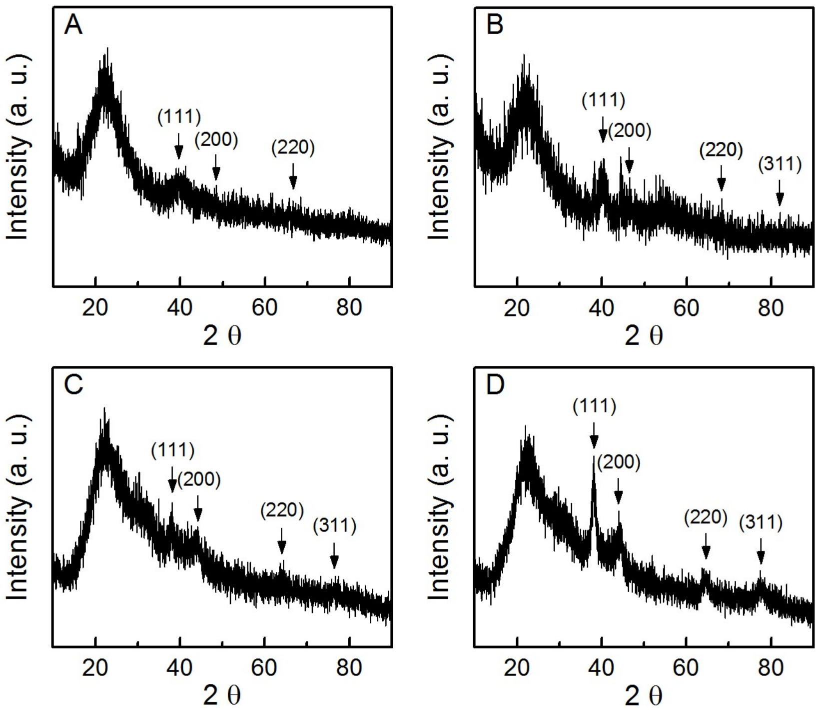


**Figure S6.** XRD patterns of Pt/DA-SBA-15 (A), Pd/DA-SBA-15 (B), Ag/DA-SBA-15 (C) and Au/DA-SBA-15 (D).

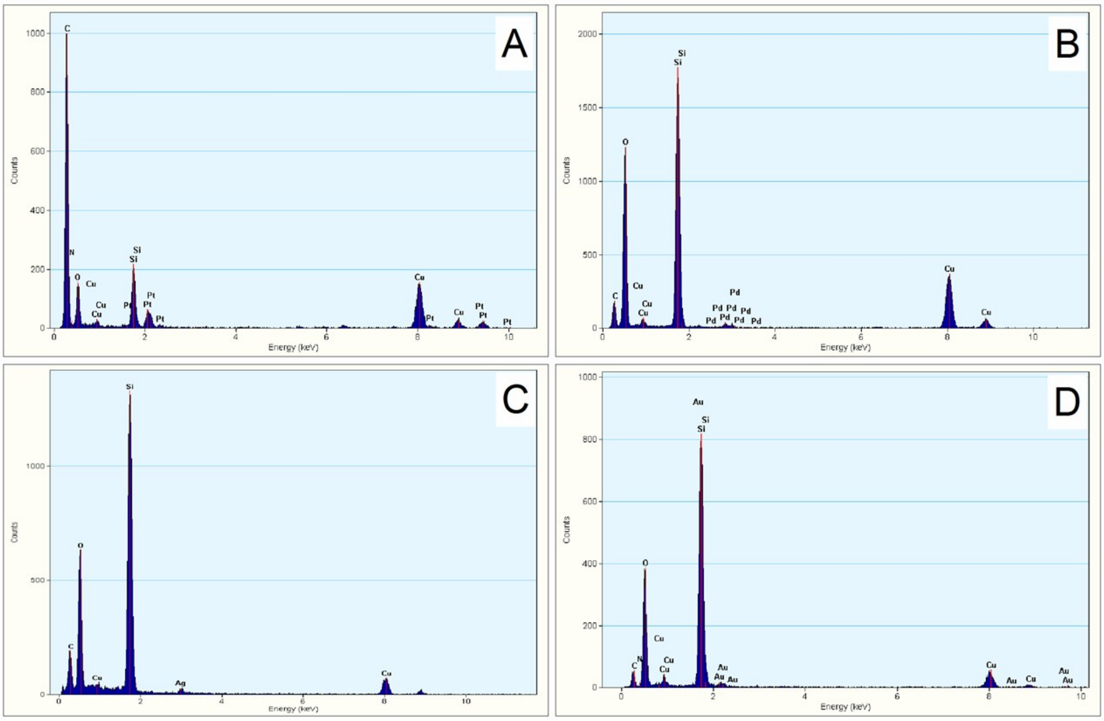


**Figure S7**. EDS spectra of Pt/DA-SBA-15 (A), Pd/DA-SBA-15 (B), Ag/DA-SBA-15(C) and Au/DA-SBA-15(D)

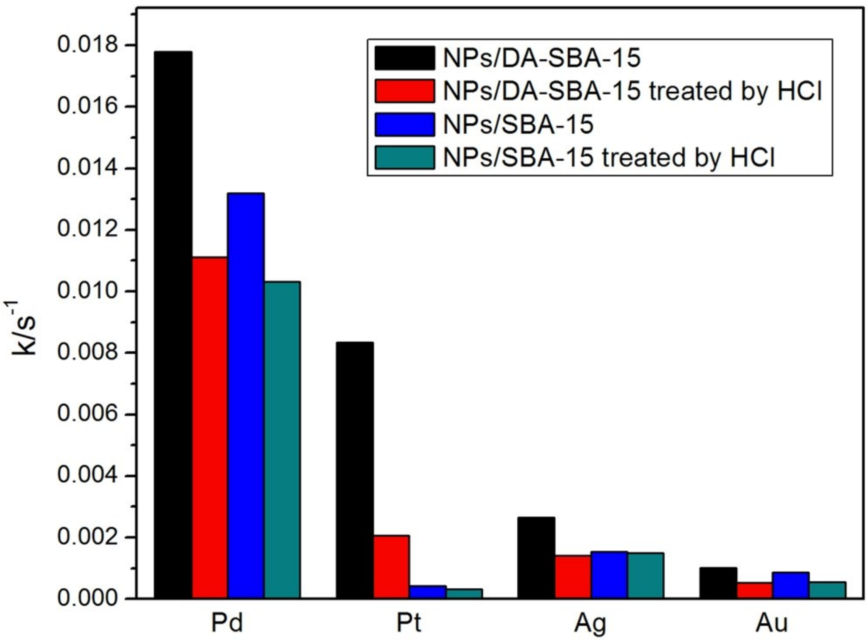


**Figure S8**. Activity changes of various catalysts treated in acidic condition of 1M HCl for 12h.

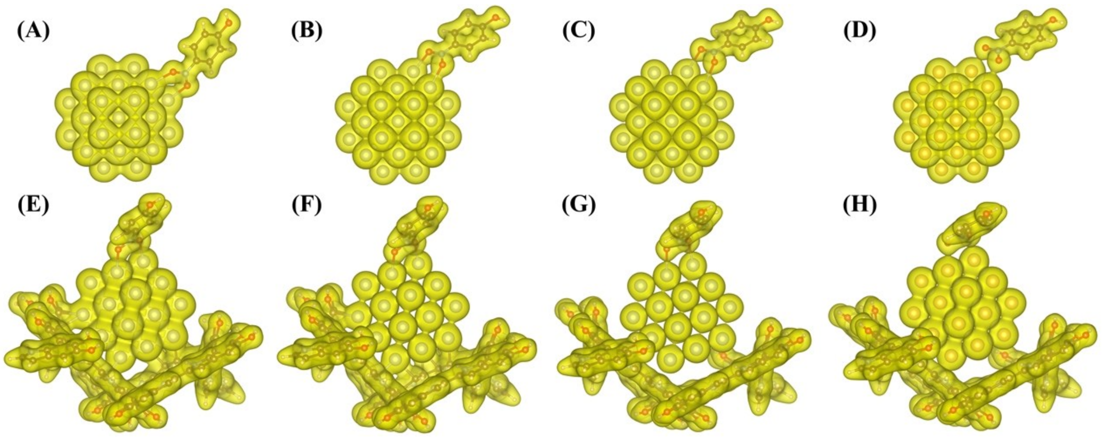


**Figure S9.** Charge density plots (isosurface value = 0.04 e/Bohr$^3$) of 4-NP molecule adsorbed on bare Pt (A), Pd (B), Ag (C), Au (D), and PDA supported Pt (E), Pd (F), Ag (G), and Au (H).

**Table S1**. Comparison of the rate constant values of various catalysts for the reduction of 4-NP by $NaBH_4$.

| Catalyst | Temperature / K | Concentration of 4-NP / mM | Rate constant ($k$) [a] / $10^{-3}$ $s^{-1}$ | $\frac{k}{c^b}$ / $s^{-1}$·m·$mol^{-1}$·L | Reference |
|---|---|---|---|---|---|
| Pt/DA-SBA-15 | RT | 0.1 | 8.35 | 8.35×$10^{-1}$ | This study |
| Pd/DA-SBA-15 | RT | 0.1 | 17.80 | 1.78 | This study |
| Ag/DA-SBA-15 | RT | 0.1 | 2.66 | 2.66×$10^{-1}$ | This study |
| Au/DA-SBA-15 | RT | 0.1 | 1.01 | 1.01×$10^{-1}$ | This study |
| Pt/SBA-15 | RT | 0.1 | 0.43 | 4.3×$10^{-2}$ | This study |
| Pd/SBA-15 | RT | 0.1 | 13.20 | 1.32 | This study |
| Ag/SBA-15 | RT | 0.1 | 1.53 | 1.53×$10^{-1}$ | This study |
| Au/SBA-15 | RT | 0.1 | 0.87 | 8.7×$10^{-2}$ | This study |
| CNC@PDA-AgNPs | RT | 0.12 | 4.26 | 2.28×$10^{-1}$ | (*1*) |
| AgNPs | RT | 0.12 | 0.76 | 4.07×$10^{-2}$ | (*1*) |
| Ag(5wt%)@SBA-15 | RT | 0.051 | 1.78 | 1.68×$10^{-1}$ | (*2*) |
| Ag(10wt%)@SBA-15 | RT | 0.051 | 12.70 | 6.04×$10^{-1}$ | (*2*) |
| micron-$SiO_2$@nano-Ag | 295 | 0.1 | 3.56 | 3.58×$10^{-3}$ | (*3*) |
| Ag(E)–$SiO_2$ | 278 | 0.45 | 10.60 | 2.72×$10^{-3}$ | (*4*) |
| GMS[c] | RT | 10 | 3.50 | 4.62×$10^{-1}$ | (*5*) |
| Au@$SiO_2$ core/shell | RT | 1.13 | 0.46 | 8.63×$10^{-4}$ | (*6*) |
| Au@$SiO_2$ yolk/shell-104 | RT | 1.13 | 14.00 | 2.62×$10^{-2}$ | (*6*) |
| Au@$SiO_2$ yolk/shell-67 | RT | 1.13 | 5.60 | 1.05×$10^{-2}$ | (*6*) |

| | | | | | |
|---|---|---|---|---|---|
| Au@$SiO_2$ yolk/shell-43 | RT | 1.13 | 3.90 | $7.32×10^{-3}$ | (*6*) |
| Pd/SBA-15 | RT | 0.1 | 12.00 | $1.92×10^{-1}$ | (*7*) |
| Pt30-G4-PS15 | RT | 0.15 | 0.20 | $2.68×10^{-3}$ | (*8*) |
| Fe@$SiO_2$/Pt NCs | RT | 0.19 | 1.50 | 1.07 | (*9*) |
| Fe@$SiO_2$/Au NCs | RT | 0.19 | 0.083 | $5.20×10^{-2}$ | (*9*) |
| $Fe_3O_4$/PDA@Ag III | RT | 0.18 | 10.00 | $8.63×10^{-2}$ | (*10*) |
| PDA-AuNPs | RT | 50 | 0.95 | $5.72×10^{-2}$ | (*11*) |
| MHNTs–PDA–Au | RT | 0.049 | 7.33 | $7.52×10^{-1}$ | (*12*) |
| AuNPs/$Fe_3O_4$@PDA-P1 | RT | 0.1 | 2.83 | $3.18×10^{-1}$ | (*13*) |
| AuNPs/$Fe_3O_4$@PDA-P2 | RT | 0.1 | 5.66 | $6.36×10^{-1}$ | (*13*) |
| AuNPs/$Fe_3O_4$@PDA-P3 | RT | 0.1 | 6.67 | $7.49×10^{-1}$ | (*13*) |
| Graphene/PDA-Au2 | RT | 0.033 | 3.75 | $1.77×10^{-2}$ | (*14*) |
| G-PDA-Au-2 | RT | 0.099 | 2.10 | $2.36×10^{-1}$ | (*15*) |
| Pd/PDA | RT | 0.1 | 0.12±0.08 | 3.56±2.39 | (*16*) |
| graphene-PDA-Pd | RT | 0.067 | 4.71 | $1.50×10^{-1}$ | (*17*) |
| Pt-PDA/RGO, | RT | 0.1 | 3.43 | $3.43×10^{-1}$ | (*18*) |
| Au-PDA/RGO | RT | 0.1 | 2.00 | $2×10^{-1}$ | (*18*) |
| $Fe_3O_4$@PDA–Pt | RT | 0.029 | 2.30 | $2.80×10^{-1}$ | (*19*) |
| Pt NPs | RT | 0.1 | 0.87 | $2.63×10^{-1}$ | (*20*) |
| Pt NCs | RT | 0.1 | 1.60 | $3.10×10^{-4}$ | (*21*) |
| Co–Pt NCs | RT | 0.1 | 3.30 | $1.29×10^{-1}$ | (*21*) |
| Ni–Pt core–shell NCs | RT | 0.1 | 1.60 | $7.41×10^{-2}$ | (*21*) |
| Pt NPs | RT | 1.33 | 3.67 | $6.01×10^{-2}$ | (*22*) |
| $Fe_3O_4$@C@Pt | RT | 0.05 | 21.9 | 1.22 | (*23*) |
| $Fe_3O_4$@C@Pd | RT | 0.05 | 18.0 | 1.00 | (*23*) |
| $SiO_2$–G1–Pt | RT | 0.083 | 7.92 | 1.10 | (*24*) |
| P-Pt NPs | RT | 0.11 | 30.00 | $2.66×10^{-2}$ | (*25*) |
| P-Pd NPs | RT | 0.11 | 57.00 | $2.69×10^{-2}$ | (*25*) |
| CNT-Pd | RT | 1.0 | 6.27 | $1.02×10^{-2}$ | (*26*) |
| $Fe_xO_y$/Pd@m$SiO_2$ | RT | 0.058 | 0.89 | 5.49×10-1 | (*27*) |
| Pd-FG | RT | 0.1 | – | $6.36×10^{-2}$ | (*28*) |
| Pd@$Fe_2O_3$@$SiO_2$ | RT | 0.098 | – | $1.10×10^{-2}$ | (*29*) |
| rGS/$Fe_2O_3$-Pd/NCS | RT | 0.12 | 2.72 | 2.02 | (*30*) |
| Pd@g-$C_3N_4$-N | RT | 0.71 | 6.35 | 5.42 | (*31*) |
| PS/PANI/Pd | RT | 1.46 | 12.90 | 2.80 | (*32*) |
| Ag NPs | RT | 0.1 | 4.47 | $1.50×10^{-3}$ | (*33*) |
| Ag NPs-5.75nm | RT | 0.1 | 2.13 | $1.53×10^{-1}$ | (*34*) |
| $Fe_3O_4$@$SiO_2$–Ag | RT | 0.061 | 7.67 | $4.85×10^{-2}$ | (*35*) |
| Ag-NP/C | RT | 0.047 | 1.69 | $9.83×10^{-4}$ | (*36*) |
| CNFs/AgNPs | RT | 0.06 | 4.6 | $3.52×10^{-1}$ | (*37*) |

| | | | | | |
|---|---|---|---|---|---|
| Ag submicroparticles | RT | 0.048 | 4.60 | 1.06 | (*38*) |
| Ag/ $Fe_xO_y$ NPs | 303.15 | 0.1 | 2.38 | $1.52\times10^{-1}$ | (*39*) |
| Au NPs | RT | 0.1 | 0.54 | $0.11\times10^{-1}$ | (*40*) |
| Au NPs | RT | 0.1 | 1.80 | $3.46\times10^{-4}$ | (*41*) |
| Au-56nm | RT | 0.066 | 0.10 | $2.44\times10^{-2}$ | (*42*) |
| Au(2)/$TiO_2$ | RT | 0.087 | 1.45 | $4.97\times10^{-1}$ | (*43*) |
| Au NPs | RT | 0.50 | 1.00 | $7.25\times10^{-1}$ | (*44*) |
| Au NPs | RT | 0.07 | 2.60 | $5.18\times10^{-1}$ | (*45*) |
| GAAu-MNP | RT | 0.10 | 6.48 | $4.32\times10^{-1}$ | (*46*) |
| Au NPs | RT | 0.20 | 1.50 | $7.50\times10^{-4}$ | (*47*) |
| Au NPs | RT | 0.10 | 12.47 | $7.77\times10^{-2}$ | (*48*) |
| Au NPs | RT | 0.20 | 1.86 | $9.30\times10^{-2}$ | (*49*) |
| Ag NPs | RT | 0.20 | 4.06 | $4.06\times10^{-2}$ | (*49*) |
| $Fe_3O_4$@$SiO_2$-Au@m$SiO_2$ | RT | 0.24 | 5.83 | $3.73\times10^{-2}$ | (*50*) |
| Au/PDDA/NCC | RT | 0.05 | 5.10 | $6.93\times10^{-2}$ | (*51*) |
| Au/graphene | RT | 0.093 | 3.17 | 7.81 | (*52*) |
| GO-$Fe_3O_4$-Au NPs | RT | 0.10 | 32.20 | 4.32 | (*53*) |
| Au Capsule | RT | 0.21 | 7.83 | $2.40\times10^{-2}$ | (*54*) |

[a] The value of *k* depends on catalyst amount.
[b] The concentration of noble metal in the reaction system. The metal content of the samples were measured by ICP-OES, EDX or calculated according to the catalyst synthesis process.
[c] GMS represented gold NPs intercalated into the walls of mesoporous silica.

## Reference


1. J. Tang, Z. Shi, R. M. Berry, K. C. Tam, Mussel-Inspired Green Metallization of Silver Nanoparticles on Cellulose Nanocrystals and Their Enhanced Catalytic Reduction of 4-Nitrophenol in the Presence of β-Cyclodextrin. *Industrial & Engineering Chemistry Research* **54**, 3299 (2015).
2. B. Naik, S. Hazra, V. S. Prasad, N. N. Ghosh, Synthesis of Ag nanoparticles within the pores of SBA-15: an efficient catalyst for reduction of 4-nitrophenol. *Catalysis Communications* **12**, 1104 (2011).
3. M. Wang, D. Tian, P. Tian, L. Yuan, Synthesis of micron-$SiO_2$@nano-Ag particles and their catalytic performance in 4-nitrophenol reduction. *Applied Surface Science* **283**, 389 (2013).
4. N. Muthuchamy, A. Gopalan, K.-P. Lee, A new facile strategy for higher loading of silver nanoparticles onto silica for efficient catalytic reduction of 4-nitrophenol. *RSC Advances* **5**, 76170 (2015).
5. L. Chen, J. Hu, Z. Qi, Y. Fang, R. Richards, Gold Nanoparticles Intercalated into the Walls of Mesoporous Silica as a Versatile Redox Catalyst. *Industrial & Engineering Chemistry Research* **50**, 13642 (2011).
6. J. Lee, J. C. Park, H. Song, A Nanoreactor Framework of a Au@$SiO_2$ Yolk/Shell

Structure for Catalytic Reduction of p-Nitrophenol. *Advanced Materials* **20**, 1523 (2008).

7. J. Morère *et al.*, Deposition of Pd into mesoporous silica SBA-15 using supercritical carbon dioxide. *The Journal of Supercritical Fluids* **56**, 213 (2011).
8. H. Li, J. Lü, Z. Zheng, R. Cao, An efficient and reusable silica/dendrimer supported platinum catalyst for electron transfer reactions. *Journal of Colloid and Interface Science* **353**, 149 (2011).
9. Z. Zhang *et al.*, A highly reactive and magnetic recyclable catalytic system based on AuPt nanoalloys supported on ellipsoidal Fe@$SiO_2$. *Journal of Materials Chemistry A* **3**, 4642 (2015).
10. B. Mao, Q. An, B. Zhai, Z. Xiao, S. Zhai, Multifunctional hollow polydopamine-based composites ($Fe_3O_4$/PDA@Ag) for efficient degradation of organic dyes. *RSC Advances* **6**, 47761 (2016).
11. Y. Ni *et al.*, One-pot preparation of pomegranate-like polydopamine stabilized small gold nanoparticles with superior stability for recyclable nanocatalysts. *RSC Advances* **6**, 40698 (2016).
12. Q. Wei, R. Shi, D. Lu, Z. Lei, In situ formation of gold nanoparticles on magnetic halloysite nanotubes via polydopamine chemistry for highly effective and recyclable catalysis. *RSC Advances* **6**, 29245 (2016).
13. Y. Zhao, Y. Yeh, R. Liu, J. You, F. Qu, Facile deposition of gold nanoparticles on core–shell $Fe_3O_4$@polydopamine as recyclable nanocatalyst. *Solid State Sciences* **45**, 9 (2015).
14. J. Luo, N. Zhang, R. Liu, X. Liu, In situ green synthesis of Au nanoparticles onto polydopamine-functionalized graphene for catalytic reduction of nitrophenol. *RSC Advances* **4**, 64816 (2014).
15. J. Cao *et al.*, In Situ Synthesis of Catalytic Active Au Nanoparticles onto Gibbsite–Polydopamine Core–Shell Nanoplates. *Langmuir* **31**, 9483 (2015).
16. Y. Liu, G. Li, R. Qin, D. Chen, Surface-Engineered Polydopamine Particles as an Efficient Support for Catalytic Applications. *Langmuir* **32**, 13675 (Dec 27, 2016).
17. J.-X. Ma *et al.*, Well-dispersed graphene-polydopamine-Pd hybrid with enhanced catalytic performance. *RSC Advances* **5**, 97520 (2015).
18. W. Ye *et al.*, Green synthesis of Pt–Au dendrimer-like nanoparticles supported on polydopamine-functionalized graphene and their high performance toward 4-nitrophenol reduction. *Applied Catalysis B: Environmental* **181**, 371 (2016).
19. S.-W. Bian, S. Liu, L. Chang, Synthesis of magnetically recyclable $Fe_3O_4$@polydopamine–Pt composites and their application in hydrogenation reactions. *Journal of Materials Science* **51**, 3643 (2015).
20. Y. Jiang *et al.*, Water-dispersible $Fe_3O_4$ nanowires as efficient supports for noble-metal catalysed aqueous reactions. *Journal of Materials Chemistry A* **2**, 4779 (2014).
21. D. Varade, K. Haraguchi, Clay-supported novel bimetallic core-shell Co-Pt and Ni-Pt nanocrystals with high catalytic activities. *Physical Chemistry Chemical Physics* **16**, 25770 (2014).
22. J. H. Lee, H. Kim, Y. S. Lee, D.-Y. Jung, Enhanced Catalytic Activity of Platinum

Nanoparticles by Exfoliated Metal Hydroxide Nanosheets. *Chemcatchem* **6**, 113 (2014).
23. P. Zhang, R. Li, Y. Huang, Q. Chen, A novel approach for the in situ synthesis of Pt-Pd nanoalloys supported on $Fe_3O_4$@C core-shell nanoparticles with enhanced catalytic activity for reduction reactions. *ACS Applied Materials & Interfaces* **6**, 2671 (2016).
24. Q. Wang *et al.*, Synthesis of Pt Nanoparticles Anchored on Polyamidoamine-Modified Hollow Silica Nanospheres for Catalytic Reduction of p-Nitrophenol. *Journal of Inorganic and Organometallic Polymers and Materials* **26**, 702 (2016).
25. J. G. You, C. Shanmugam, Y. W. Liu, C. J. Yu, W. L. Tseng, Boosting catalytic activity of metal nanoparticles for 4-nitrophenol reduction: Modification of metal naoparticles with poly(diallyldimethylammonium chloride). *Journal of Hazardous Materials* **324**, 420 (2017).
26. D. K. Ji, M. Y. Choi, H. C. Choi, Catalyst activity of carbon nanotube supported Pd catalysts for the hydrogenation of nitroarenes. *Materials Chemistry & Physics* **173**, 404 (2016).
27. T. Yao, T. Cui, X. Fang, F. Cui, J. Wu, Preparation of yolk-shell $Fe_xO_y$/Pd@mesoporous $SiO_2$ composites with high stability and their application in catalytic reduction of 4-nitrophenol. *Nanoscale* **5**, 5896 (2013).
28. Z. Wang, C. Xu, G. Gao, X. Li, Facile synthesis of well-dispersed Pd–graphene nanohybrids and their catalytic properties in 4-nitrophenol reduction. *Rsc Advances* **4**, 13644 (2014).
29. L. Huang *et al.*, Iron oxide nanoparticle layer templated by polydopamine spheres: a novel scaffold toward hollow-mesoporous magnetic nanoreactors. *Nanoscale* **7**, 806 (2014).
30. T. Yao *et al.*, A simple way to prepare reduced graphene oxide nanosheets/$Fe_2O_3$-Pd/N-doped carbon nanosheets and their application in catalysis. *Journal of Colloid & Interface Science* **468**, 62 (2016).
31. F. Wei *et al.*, Synthesis of Pd/Au bimetallic nanoparticle-loaded ultrathin graphitic carbon nitride nanosheets for highly efficient catalytic reduction of p-nitrophenol. *Journal of Colloid & Interface Science* **490**, 834 (2017).
32. H. Y. Lee, S. P. Rwei, L. Wang, P. H. Chen, Preparation and characterization of core–shell polyaniline–polystyrene sulfonate@$Fe_3O_4$ nanoparticles. *Materials Chemistry & Physics* **112**, 805 (2008).
33. T. V. Thu, P. J. Ko, N. H. H. Phuc, A. Sandhu, Room-temperature synthesis and enhanced catalytic performance of silver-reduced graphene oxide nanohybrids. *Journal of Nanoparticle Research* **15**, 1 (2013).
34. K. B. Narayanan, N. Sakthivel, Heterogeneous catalytic reduction of anthropogenic pollutant, 4-nitrophenol by silver-bionanocomposite using Cylindrocladium floridanum. *Bioresource Technology* **102**, 10737 (2011).
35. Y. Chi *et al.*, Synthesis of Fe3O4@SiO2–Ag magnetic nanocomposite based on small-sized and highly dispersed silver nanoparticles for catalytic reduction of 4-nitrophenol. *Journal of Colloid & Interface Science* **383**, 96 (2012).
36. S. Tang, S. Vongehr, X. Meng, Carbon Spheres with Controllable Silver

Nanoparticle Doping. *Journal of Physical Chemistry C* **114**, 977 (2010).
37. P. Zhang *et al.*, In situ assembly of well-dispersed Ag nanoparticles (AgNPs) on electrospun carbon nanofibers (CNFs) for catalytic reduction of 4-nitrophenol. *Nanoscale* **3**, 3357 (2011).
38. B. Tang, J. Li, L. Fan, X. Wang, Facile synthesis of silver submicrospheres and their applications. *Rsc Advances* **5**, 98293 (2015).
39. J. R. Chiou, B. H. Lai, K. C. Hsu, D. H. Chen, One-pot green synthesis of silver/iron oxide composite nanoparticles for 4-nitrophenol reduction. *Journal of Hazardous Materials* **248**, 394 (2013).
40. K. B. Narayanan, N. Sakthivel, Synthesis and characterization of nano-gold composite using Cylindrocladium floridanum and its heterogeneous catalysis in the degradation of 4-nitrophenol. *Journal of Hazardous Materials* **189**, 519 (2011).
41. X. Wang *et al.*, Reduced state carbon dots as both reductant and stabilizer for the synthesis of gold nanoparticles. *Carbon* **64**, 499 (2013).
42. R. Fenger, E. Fertitta, H. Kirmse, A. F. Thünemann, K. Rademann, Size dependent catalysis with CTAB-stabilized gold nanoparticles. *Physical Chemistry Chemical Physics* **14**, 9343 (2012).
43. Y. Hao, X. Shao, B. Li, L. Hu, T. Wang, Mesoporous $TiO_2$ nanofibers with controllable Au loadings for catalytic reduction of 4-nitrophenol. *Materials Science in Semiconductor Processing* **40**, 621 (2015).
44. C. Deraedt *et al.*, Sodium borohydride stabilizes very active gold nanoparticle catalysts. *Chemical Communications* **50**, 14194 (2014).
45. X. Q. Wu, X. W. Wu, Q. Huang, J. S. Shen, H. W. Zhang, In situ synthesized gold nanoparticles in hydrogels for catalytic reduction of nitroaromatic compounds. *Applied Surface Science* **331**, 210 (2015).
46. C. C. Wu, D. H. Chen, Spontaneous synthesis of gold nanoparticles on gum arabic-modified iron oxide nanoparticles as a magnetically recoverable nanocatalyst. *Nanoscale Research Letters* **7**, 317 (2012).
47. A. Zinchenko, Y. Miwa, L. I. Lopatina, V. G. Sergeyev, S. Murata, DNA hydrogel as a template for synthesis of ultrasmall gold nanoparticles for catalytic applications. *ACS Applied Materials & Interfaces* **6**, 3226 (2014).
48. Y. C. Chang, D. H. Chen, Catalytic reduction of 4-nitrophenol by magnetically recoverable Au nanocatalyst. *Journal of Hazardous Materials* **165**, 664 (2009).
49. A. Gangula *et al.*, Catalytic reduction of 4-nitrophenol using biogenic gold and silver nanoparticles derived from Breynia rhamnoides. *Langmuir* **27**, 15268 (2011).
50. Y. Deng *et al.*, Multifunctional Mesoporous Composite Microspheres with Well-Designed Nanostructure: A Highly Integrated Catalyst System. *Journal of the American Chemical Society* **132**, 8466 (2010).
51. E. Lam, S. Hrapovic, E. Majid, J. H. Chong, J. H. Luong, Catalysis using gold nanoparticles decorated on nanocrystalline cellulose. **4**, 997 (2012).
52. J. Li, C. Y. Liu, Y. Liu, Au/graphene hydrogel: Synthesis, characterization and its use for catalytic reduction of 4-nitrophenol. *Journal of Materials Chemistry* **22**, 8426 (2012).
53. J. Hu *et al.*, A highly efficient catalyst: In situ growth of Au nanoparticles on

graphene oxide–$Fe_3O_4$ nanocomposite support. *Chemical Engineering Journal* **236**, 1 (2014).
54. J. Xu *et al.*, Synthesis of Au and Pt Hollow Capsules with Single Holes via Pickering Emulsion Strategy. *Journal of Physical Chemistry C* **119**, 28055 (2015).